Polish J. Chem., **75**, 719–732 (2001)

Synthesis and Surface Acidity of Amorphous Fluorine-Containing Aluminium Borates

by S.Ya. Brichka* and V.V. Brei

Institute of Surface Chemistry, National Academy of Sciences of Ukraine, Prospect Nauky 31, 03022 Kyiv, Ukraine

(Received October 18th, 2000; revised manuscript December 20th, 2000)

A series of fluorine-containing aluminium borate samples with Al_2O_3/B_2O_3 = 3 and HF/B_2O_3 = 0.05–0.50 molar ratios has been synthesized by an impregnation method using NH_4F. The materials obtained are amorphous up to 840–1130 K. Their thermal transformations were investigated by DTA and MSA. There are Lewis and Brönsted acid sites present in these samples. The very strong Lewis sites are due to formation of trigonal B^{3+}, bonded with F^- on the surface of fluorine-containing aluminium borates. Dehydration of isopropyl alcohol was used as a probe reaction to measure the acidity. The results of measurements have shown that these materials were more acidic and catalytically active than the starting aluminium borate.

Key words: fluorine-containing aluminium borate, synthesis, thermal transformations, acidity

Aluminium borates and related compounds have attracted considerable attention in heterogeneous catalysis, being grouped into classes of native borates (such as a rare mineral jeremejevite ($Al_6[BO_3]_5(OH)_3$)) and synthetic aluminium borates that are much more abundant [1–5]. Crystalline aluminium borates with transition metals [6–9] possess useful magnetic and catalytic properties. For example, good catalytic activities are characteristic of mixed catalysts on the basis of aluminium and boron oxides [10–12]. Surface characterization of alumina-boria samples was investigated [13]. It has been found that under hydrothermal conditions crystalline aluminium borates are synthesized [14,15], but no data on the surface chemistry of these materials are available. Amorphous aluminium borates are acidic materials of high technological interest in catalysis [16–18]. They possess a high surface area and microporosity, typical for zeolites. The materials are stable up to 1073 K and exhibit both Lewis and Brönsted acid sites. One of the limitations of these compounds is considered to be their lower catalytic activity (for example in an alcohol dehydration) in comparison with γ-Al_2O_3. Obviously, the improvement of catalytic properties of the amorphous aluminium borates would expand their practical application.

*Author for correspondence.

Recently, a new class of halogen-containing aluminium borates has been hydrothermally synthesized [19–24]. The materials exhibit a unique three-dimensional framework structure, consisting of space units built up by trigonal and tetrahedral boron ions (B^{3+}) and octahedral aluminium ions (Al^{3+}). The fact that the novel aluminium borate structure involves such components as halogen anions (F^-, Cl^-, Br^-) results in useful catalytic properties and peculiar surface acidity. These characteristics are subject of research at our laboratory, and the results achieved when studying one of such compounds, namely aluminium-boron oxofluoride, have already been described [23]. In the structure of this compound there are strong Lewis acid sites and base sites, which exhibit a high activity in the reaction of dehydrogenation of isopropyl alcohol to acetone. In our opinion, the most promising acid-base properties are characteristic of a number of halogen-containing aluminium borates and first of all of fluorine-containing compounds.

This paper reports results on the synthesis of fluorine-containing amorphous aluminium borates. The thermal stability of these substances is examined in detail in comparison with the starting aluminium borate. Of particular interest is the relation between the surface structure of the compounds and their catalytic activities.

EXPERIMENTAL

Synthesis. Aluminium borate samples were synthesized as described in [18]. A mixture with the molar composition $3Al_2O_3$:$1B_2O_3$:3.5glycerol:$30H_2O$ was prepared from $Al(NO_3)_3 \cdot 9H_2O$, boric acid, glycerol, and water. Dissolution of the ingredients at room temperature led to formation of a single liquid phase. When the aqueous solution was heated to 363 K, reactions between its components took place, leading to a white solid substance. This synthesized compound will be denoted as the starting aluminium borate (AB). It was heat-treated in air at 450 K for 1 h and at 673 K for 0.5 h in order to attain oxidation of the organic reactants and a more complete removal of nitrogen oxides. The aluminium borates synthesized were modified by fluorine anions (F^-) in the following procedure: The starting sample was impregnated with an aqueous solution of ammonia fluoride (NH_4F) for 20 h at room temperature and dried at 383 K. The F^- concentration varied over a wide range, governed by the NH_4F:B_2O_3 ratio from 0.05 to 3. Depending on the solution concentration, the pH values of the reaction mixture ranged from a neutral pH ≈ 6.8 to a basic pH = 7.5–8.6. The reaction that takes place is:

$$Al_3BO_6 + nNH_4F \rightarrow Al_3BO_{6-n/2}F_n + nNH_3 + (n/2)H_2O \quad (1)$$

The results of the synthesis of the fluorine-containing aluminium borates and the chemical composition of the solid products are summarized in Table 1. The sample with the molar ratio Al_2O_3:B_2O_3 = 3:1 was chosen because of its high surface area (more than 400 $m^2\ g^{-1}$), the most narrow pore-size distribution, and other characteristics that make it a typical representative of amorphous aluminium borates.

Characterization methods. DTA was performed on a Q-1500D thermogravimetric analyzer with a heating rate 10 K min^{-1} from 298 to 1273 K. X-ray powder diffraction (XRD) patterns were recorded on a DRON-2M diffractometer (Co Kα radiation). Surface area was determined by BET of N_2 at 77 K. Infrared spectra were recorded at room temperature on a Perkin-Elmer 325 spectrometer using a KBr pellet at a resolution of 2 cm^{-1}. For the acidity study, the samples were pressed into a self-supporting wafer and evacuated at 573 K for 0.5 h in a quartz cell. After cooling to room temperature the adsorption of probe molecules (pyridine, deuteroacetonitrile (CD_3CN) and benzonitrile (PhCN)) was performed by exposing the samples for 0.5 h. The spectra were recorded for the samples treated for 0.5 h at various temperatures. The

adsorbates were used after repeated freeze-pumpthaw cycles. The IR experiments were carried out under similar conditions to enable a correct comparison between corresponding concentrations of the acid sites. The surface acidity was studied by temperature-programmed desorption of ammonia (TPD of NH_3) and temperature-programmed reaction (TPR) of dehydration of isopropyl alcohol to propylene with a mass spectrometric control, according to the following procedure: a sample of about 4–6 mg was placed in a quartz cell that is evacuated at 573 K. Adsorption of NH_3 and isopropyl alcohol was carried out at room temperature with the subsequent evacuation. The temperature was raised from 293 to 873 K with a linear heating rate of 10 K min^{-1}. To monitor the desorption products leaving the sample, the effluent was analysed for the presence of NH_3 (m/z = 17 amu) and H_2O (m/z = 18 amu). In the case of the TPR technique, the decomposition products of propylene (m/z = 42 amu) and acetone (m/z = 43 amu) were recorded. The spectra were normalized to the same conditions.

Table 1. Synthesis parameters, composition and surface area of solid products.

Sample	Composition of the reaction mixture (molar ratio), HF/AB	F^- content of solid product/wt.%	XRD analysis of solid product	N_2 surface area / m^2 g^{-1}
AB	–	–	Amorphous	314
ABF005	0.05	< 1	Amorphous	304
ABF01	0.1	~1.5	Amorphous	258
ABF05	0.5	5	Amorphous	225
ABF1	1	9	Amorphous	200
ABF2	2	16	Amorphous + $(NH_4)_3AlF_6$	–
ABF3	3	23	Amorphous + $(NH_4)_3AlF_6$ +AlF_3	–

RESULTS AND DISCUSSION

Thermal properties. The DTA runs on all amorphous fluorine-containing aluminium borates show one endothermic and two exothermic peaks. The thermograms recorded for AB, ABF005, and ABF1 are presented in Fig. 1. The endothermic peak at 413–438 K can be attributed to desorption of physically sorbed water. Going from ABF005 to ABF1 the intense peak of the first exotherm occurred between 573 and 633 K gradually increases. In the case of the aluminium borate without F^- in its structure, this peak is not observed. The position of the maximum of the second exothermic peak at 840–1130 K varies significantly, depending on the sample composition as shown in Fig. 2. With the increasing content of F^-, the temperature maximum (T_{max}) is shifted by 300 K towards lower temperature and the thermal effect diminishes (Fig. 1). It should be noted that in the case of low contents of F^- the exothermic maximum position changes slightly.

XRD analyses of all samples allow us to assign the high-temperature exothermic effect to formation of a crystalline phase of aluminium borate. Fig. 3 gives the X-ray powder diffraction patterns of the ABF01 as synthesized and calcined at different temperatures. The X-ray pattern of the sample treated at 573 K for 1 h does not show any diffraction peaks, typical for amorphous materials. After calcination of the speci-

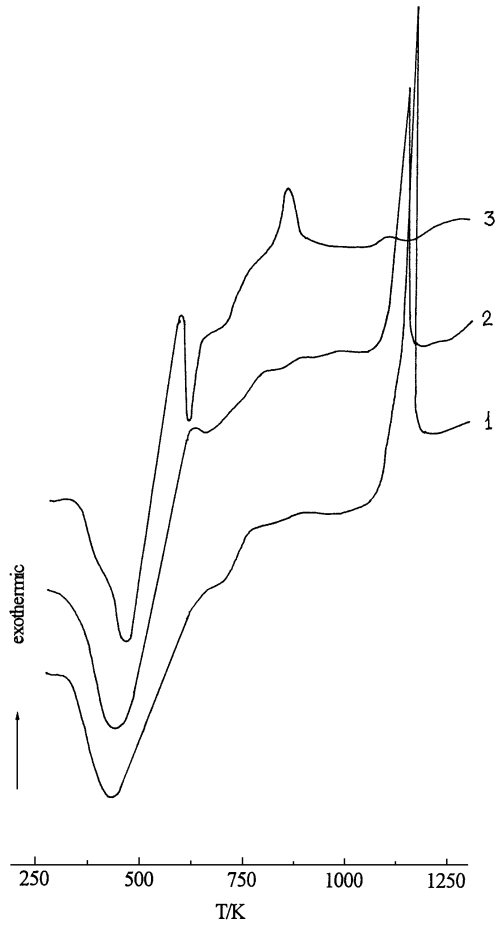

Figure 1. Differential thermoanalysis curves for AB (**1**), ABF005 (**2**) and ABF1 (**3**).

men at 1123 K, the XRD analysis presents a crystalline phase. In the case of mixed oxides of aluminium [25] the formation of a crystalline phase takes place between 1073–1173 K as it was the case for our starting material.

Fig. 4 shows TG-TPD patterns for ABF01. The thermal analysis results indicate that the amorphous fluorine-containing aluminium borates have three main stages of mass loss as well as three thermal effects. The desorption mass spectrometric analysis of the gas phase over the fluorine-containing samples at elevated temperatures shows that the main components of the decomposed products are H_2O, $(BOF)_3$, and HF.

The TPD profile of H_2O for the samples in the 300–473 K range exhibits a broad peak corresponding to the first mass loss in its TG curve. With the increasing content of F^- in the aluminium borates, T_{max} of the H_2O desorption is shifted by 40 K towards the high-temperature region in comparison with the starting specimen. The TPD profiles of H_2O (Fig. 4) show also a desorption peak at 653 K. On the basis of our IR experiments on the physically sorbed H_2O, it is evident that its subsequent desorption

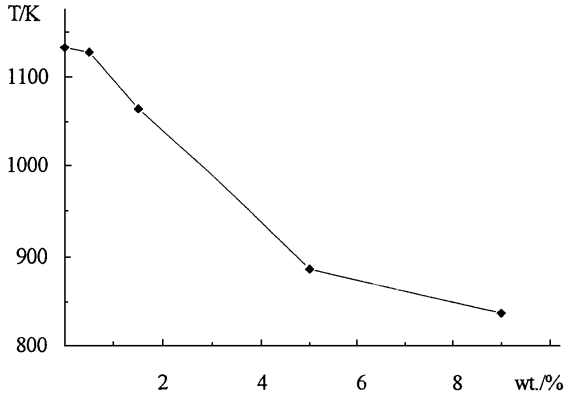

Figure 2. Effect of the fluorine content on the temperature of transitions from the amorphous state to crystalline state for the starting aluminium borate and fluorine-containing samples.

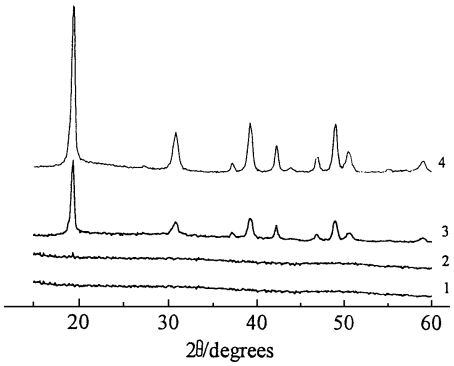

Figure 3. X-ray patterns for ABF01 heat-treated at different temperatures: 300 K (**1**), 573 K (**2**), 1123 K (**3**) and 1273 K (**4**).

from the samples was controlled by the vibration band of water molecules at 1640 cm^{-1}. The band disappeared after the sample evacuation at 473 K for 0.5 h. Consequently, this water was formed as a result of dehydroxylation. The hydroxylated form of the materials is converted to the oxide form.

The second peak of mass losses for all the fluorine-containing samples is observed in the 573–623 K range. The TPD spectra of $(BOF)_3$ have a T_{max} of about 663 K (Fig. 4). This peak of mass losses is assigned to the release of $(BOF)_3$ occurring with the exothermic effect. The formation of BF_3 (m/z = 49 amu) was not detected. The X-ray powder diffraction pattern of the ABF01 calcinated at 573 K shows it to be an amorphous product. Though the fluorine-containing aluminium borates are partially destroyed at about 573 K, the amorphous state of the samples is preserved.

The TG curves, recorded only for the fluorine-containing aluminium borates, reveal the last distinct mass loss at 833–1133 K. The transformation of the samples occurs during the course of crystallization of the fluorine-containing compounds. The

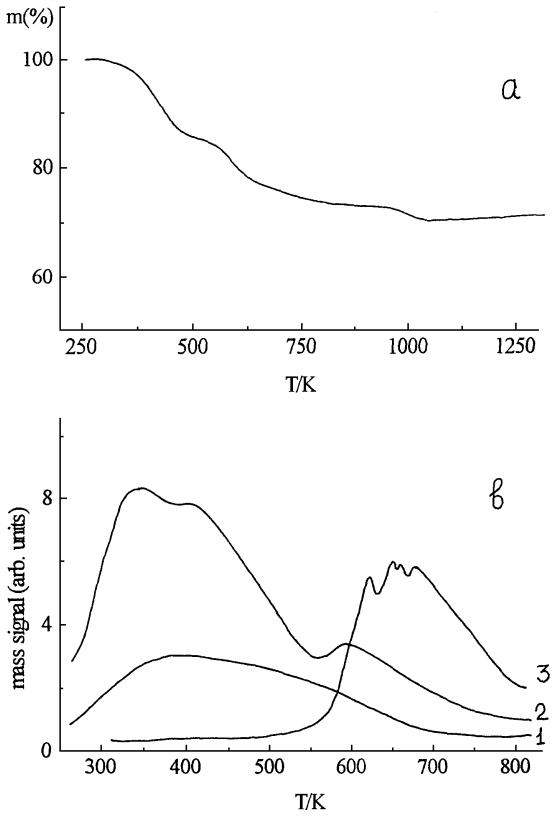

Figure 4. TG curve for ABF01 (*a*) and corresponding TPD profiles for HF ($m/z = 20$ amu) (**1**), H_2O ($m/z =$ 17 amu; at a 1:20 scale) (**2**) and $(BOF)_3$ ($m/z = 46$ amu) (**3**).

crystallization of the starting aluminium borate is not accompanied by a mass loss and seems to take place due to the absence of F^- in the structure of the sample. During the crystallization of the fluorine-containing aluminium borates at high temperatures, the mass loss can be interpreted as formation of gaseous boron-containing products. It is known that the reaction

$$2AlF_3 + B_2O_3 = 2BF_3 + Al_2O_3 \quad (2)$$

is reversible. Above 773 K the reaction leads to formation of BF_3. It is evident that above 773 K the fluoride anions, that form covalent bonds with Al^{3+}, enter into a reaction with B_2O_3 leading to volatile compounds of boron. The influence of thermal treatment on the structure of the fluorine-containing aluminium borates was studied by IR. Fig. 5 shows the IR spectra of ABF01 after the calcination between 373–1273 K range for 2 h. The spectra were recorded using pressed disks of KBr. It is seen that the fluorine-containing samples have an IR spectrum, which is similar to that observed for the region of skeleton vibrations of the starting aluminium borate. The poorly re-

solved absorption bands near ν_{as} = 680 cm^{-1} and ν_s = 580 cm^{-1} are characteristic of Al^{3+} in an octahedral environment, and an absorption band at 700–850 cm^{-1} indicates the presence of tetrahedral Al^{3+} ions [26]. The ^{27}Al MAS NMR data of [18] corroborate the above conclusion about the IR spectrum features. In the structure of the amorphous aluminium borates exist also five-coordinated atoms with a resonance observed at 30 ppm. According to [16], this signal is related to a structural fragment of $Al(OB)_4$ of four-coordinated Al^{3+}. The bands at 1450–1240 cm^{-1} and at 1200–900 cm^{-1} for the stretching vibrations of B^{3+} are characteristic of trigonal and tetrahedral boron respectively [17,26,27]. In addition, with increasing temperature of the treatment of ABF01, one can observe the following changes in the IR spectra: (i) redistribution of intensities of the absorption bands of trigonal and tetrahedral B^{3+}; the absorption attributed to the first group of ions decreases, while the absorption assigned to the second group is not changed; (ii) splitting of the bands ascribed to Al^{3+} ions that are seen to exist in the different coordination states.

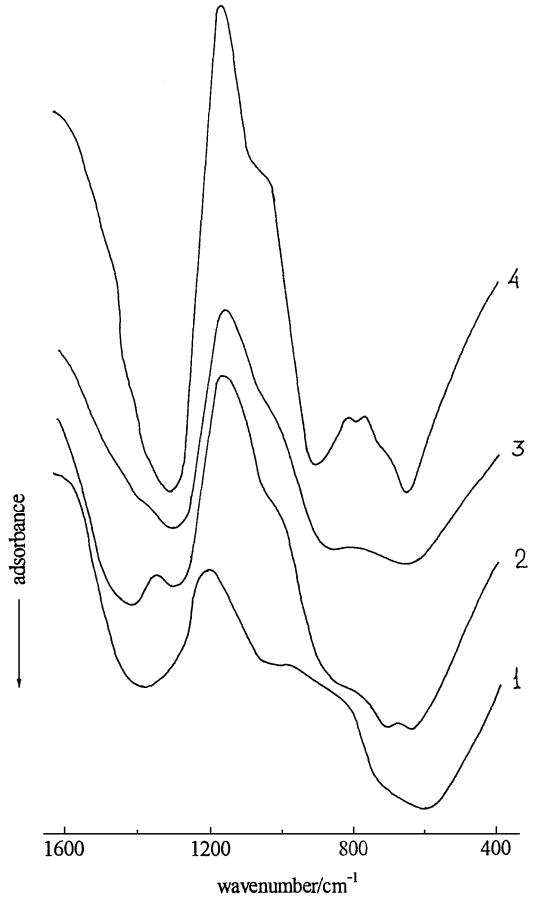

Figure 5. IR spectra for ABF01 heat-treated at different temperatures: 373 K (**1**), 773 K (**2**), 1123 K (**3**) and 1273 K (**4**).

Surface characterization. In order to characterize the adsorption sites of the aluminium borate surface, the IR spectra have been examined for changes related to pyridine adsorption. The spectrum of the original sample, outgassed at 673 K, show a band at 2348 cm^{-1} that has been assigned to CO_2 introduced into the particles during the preparation. In the 1530–1200 cm^{-1} region the transmission is negligible, due to stretching vibrations of the trigonal B^{3+}. First of all, an attempt has been made to consider the spectra in the 1540–1650 cm^{-1} region. It should be noted that the identification of Lewis acid sites (L-sites) in the presence of Brönsted acid sites (B-sites) in the 1450–1460 cm^{-1} region is usually performed using pyridine as probe molecules, because otherwise some errors in the interpretation of the spectra can arise [28].

After the adsorption of pyridine, the IR spectra of all the aluminium borates exhibit adsorption bands at 1545, 1590, 1608, 1618, and 1640 cm^{-1}. After the vacuum treatment of the samples at room temperature, the band at 1590 cm^{-1} disappears, it is therefore assigned to physically sorbed pyridine. The narrow intense bands at 1545 and 1640 cm^{-1} are due to the vibrations of pyridinium ions, which points to the presence of B-sites. The bands at about 1608 and 1618 cm^{-1} are assigned to pyridine molecules coordinatively bonded at L-sites of two types. The spectrum of pyridine adsorbed on the starting aluminium borate has been discussed elsewhere [17].

With the view of conducting a more detailed investigation of the L-sites of the synthesized samples we used CD_3CN and PhCN as probe molecules. Nitriles are known to interact with strong B-sites to produce only hydrogen bonds [29]. They are widely used for identification of L-sites. In our opinion, PhCN has an advantage over CD_3CN, because the intensity of its ν_{CN} band is higher than that in the aliphatic nitriles [28,30].

The spectra of CD_3CN adsorbed on the starting aluminium borate and on ABF1 are similar. In the CN spectral region there are four bands, namely at 2270, 2300, 2310, and 2348 cm^{-1}. The band at 2348 cm^{-1} is due to CO_2 and that at 2270 cm^{-1} is attributed to physically sorbed CD_3CN (the band disappears after the evacuation of the samples at room temperature). The bands at 2300 and 2310 cm^{-1} are caused by the interaction of CD_3CN with L-sites. These two bands are related to the L-sites, whose type is identical to that identified when conducting the above-described experiments with the pyridine adsorption on the corresponding samples. The spectra recorded in the case of the PhCN adsorption at room temperature on all the synthesized samples are compared in Fig. 6. The spectra of the fluorine-containing samples differ from those recorded on the CD_3CN adsorption. The spectrum of the starting aluminium borate, after the PhCN adsorption, has four bands, as in the case of the spectrum for the CD_3CN adsorption. The bands at 2298 and 2310 cm^{-1} are due to the interaction with two types of L-sites. Simultaneously in the spectrum of the ABF1 after the PhCN adsorption five bands exist (Fig. 6). In addition to the bands attributed to CO_2 and physically sorbed probe molecules, there are very well-resolved bands at 2302, 2315, and 2336 cm^{-1}. Such a difference can be interpreted in terms of the fact that the band for the CD_3CN adsorption on new L-sites is obscured by the CO_2 adsorption band at 2348 cm^{-1}. Thus, the fluorine-containing aluminium

borates have three types of L-sites on the surface. All the spectroscopic data are summarized in Table 2.

It is evident that the above-described L-sites can appear on the surface of the synthesized samples only in the presence of coordinatively unsaturated Al^{3+} and B^{3+}. It has already been shown that the samples contain five- and four-coordinated Al^{3+} and three-coordinated B^{3+}. In the adsorption of PhCN the bands at 2300 cm^{-1} and 2310 cm^{-1} can be related to L-sites of five- and four-coordinated Al^{3+} respectively. The three-coordinated B^{3+} in the environment of oxygen anions do not possess the property of L-sites observed in the case of the reaction with such bases as pyridine (C_5H_5N), deuteroacetonitrile (CD_3CN) [17,20,22,24]. Before the reaction with pyridine, trigonal B^{3+} ions are situated on the plane defined by their neighbouring oxygen atoms, because this position is most advantageous [31]. When interacting with pyridine, these ions should move to tetrahedral three-dimensional positions. Since B^{3+} ions are rigidly fixed in the aluminium borate matrix, such a structural transformation seems to be energetically unfavourable.

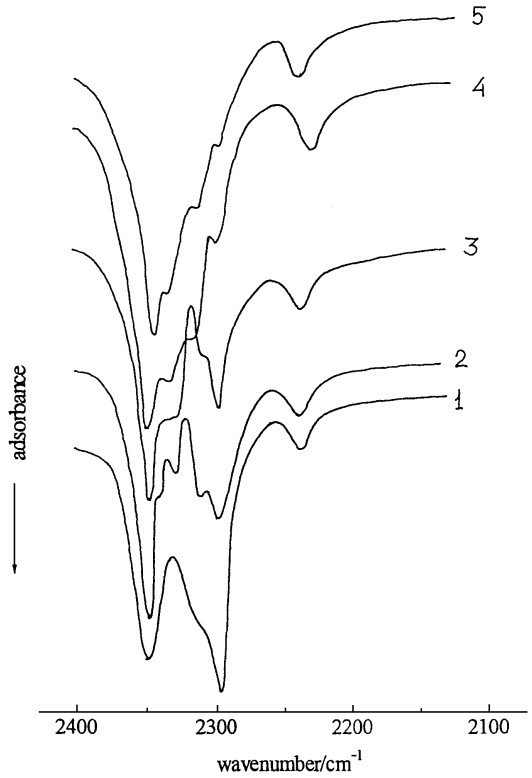

Figure 6. IR spectra for PhCN adsorbed on AB (**1**), ABF005 (**2**), ABF01 (**3**), ABF05 (**4**) and ABF1 (**5**).

Table 2. Adsorption bands of PhCN coordinatively bonded on surface of samples and suggested L-acid sites.

Sample	Bands of PhCN coordinatively bonded/cm^{-1}
AB	2296[a], 2310[b]
ABF005	2300[a], 2310[b], 2330[c]
ABF01	2300[a], 2311[b], 2330[c]
ABF05	2302[a], 2315[b], 2335[c]
ABF1	2302[a], 2315[b], 2336[c]

Suggested L-acid sites: [a] – 5-coordinated Al^{3+}, [b] – 4-coordinated Al^{3+}, [c] – 3-coordinated B^{3+} in F^- environment.

The strength of L-sites can be evaluated on a relative scale of the absorption band shift [32]. The larger is the shift, the stronger is the interaction of sites with the probe molecules, and, hence, the higher is the strength of the corresponding L-sites. The bands at 2330–2336 cm^{-1} of the adsorbed PhCN should be related to acid sites that are stronger than the coordinatively unsaturated Al^{3+}. Fluorination of the starting aluminium borate leads to formation of new acid sites, and on the basis of the shift of the absorption band for PhCN ($\Delta\nu$ = 70–76 cm^{-1}) they can be assigned to three-coordinated B^{3+} bonded with F^-.

With the increasing F^- content in the samples, the IR spectra of the adsorbed PhCN (Fig. 6) exhibit the following changes: (i) sharp decreasing of the absorption of the coordinatively bonded PhCN at ~2300 and ~2310 cm^{-1}; (ii) increasing of the absorption of PhCN at 2330–2336 cm^{-1}; (iii) shift of the position of these bands towards the high-frequency region.

The observed changes in the number and strength of L-acid sites can be explained by the following factors: It is evident that F^- acts as a base, whose reaction with acid ions 4- and 5-coordinated Al^{3+} leads to addition of HF and completion of the constructing of coordination spheres of unsaturated Al^{3+}. As a consequence, the number of L-sites decreases. 6-coordinated Al^{3+} do not form coordination complexes with benzonitrile and pyridine [17]. For samples with the higher contents of F^- the concentration of L-sites of B^{3+} substantially increases (Fig. 6).

The substitution of fluoride anions for OH^- affects the acidity of remaining acid sites of Al_2O_3 [28,33]. Similar changes have also been observed in the acidity spectrum for fluorine-containing aluminium borates. Upon the substitution of fluoride anions for surface OH^- of aluminium borate the acceptor strength of L-site increases, which is attributed to a more strong shift of the electron density from Al^{3+} to F^- and which manifests itself in the IR spectra for the adsorbed PhCN (Fig. 6), with the band of absorption of the coordinatively bonded probe being shifted by 5–6 cm^{-1} into the high-frequency region. These observations can be explained by an increase in the number of fluorine atoms neighbouring with Al^{3+} and B^{3+} in both the short-range and long-range coordination spheres. It should be noted that it is the application of PhCN but not CD_3CN as a molecular probe for samples with absorption bands in the CN region that allowed us to detect new L-acid sites.

Thus, with increasing F^- content in the samples, the concentration of the Al^{3+} L-acid sites decreases, while the concentration of the B^{3+} L-sites increases. Owing to the high electronegativity of fluorine, the strength of the all L-sites of fluorine-containing samples increases, which affects the catalytic properties.

The temperature-programmed desorption of NH_3 is known to be widely used to measure the acidity of solid catalysts [34,35]. Our experiments have shown that the TPD spectra for amorphous aluminium borates are not informative. Because of the amorphous state of samples, their TPD peaks are strongly broadened and desorption of NH_3 is observed up to 573 K. In view of this fact our investigation of surface acid-base sites and estimation of catalytic activity of the samples synthesized [35,36] were carried out by the TPR method for dehydration of isopropyl alcohol. The results achieved corroborated the presence of acid sites on the surface of all the samples. In addition, no formation of acetone over the catalysts was observed, as one would expect in the case of the presence of strong basic sites [37]. Besides, we have also stud-

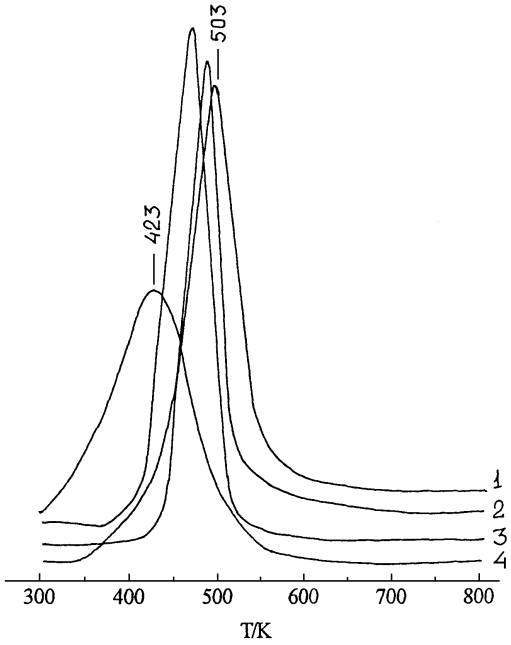

Figure 7. TPR profiles for releasing of propylene in the case of AB heat treated at different temperatures: 373 K (**1**), 473 K (**2**), 673 K (**3**) and 773 K (**4**).

ied the influence of thermal treatment of the starting aluminium borate on its catalytic activity. The corresponding spectra of dehydration of isopropyl alcohol are presented in Fig. 7. It is seen that the spectra of samples thermally treated at 373 and 473 K are similar (in both cases $T_{max} \approx 503$ K). The highest intensity of the propylene release is observed for the sample thermally treated at 673 K, with T_{max} being shifted by 30 K into the low-temperature region. The spectrum of the sample treated at 773 K exhibits

marked changes: it is strongly broadened, and the intensity of the release of propylene decreases. Therefore, the most appropriate temperature for thermal treatment of amorphous aluminium borates as catalysts is 673 K.

From the TPR spectrum of the starting aluminium borate it is evident, that the width of the propylene release interval is 100 K and T_{max} = 473 K (Fig. 8). The TPR spectra for fluorine-containing samples display more intense peaks with T_{max} from 403 to 453 K. With the increasing F^- content in the samples, T_{max} is shifted towards the low-temperature region (from 453 K for ABF005 to 433 K for ABF01 and ABF05 and to 403 K for ABF1) (see Fig. 8). The introduction of F^- into the structure of the samples leads to a shift by 20–70 K in T_{max} of the reaction of dehydration of isopropyl alcohol. The TPR spectrum for ABF005 provides evidence for a slight increase in the propylene release intensity. From the spectrum for ABF01, that possesses the highest catalytic activity, it is seen that the propylene release intensity of this sample is about ten times larger than that of the starting aluminium borate. In other samples, this intensity gradually decreases but, nevertheless, it remains higher than that characteristic of the starting aluminium borate. It should be noted that the aluminium borates

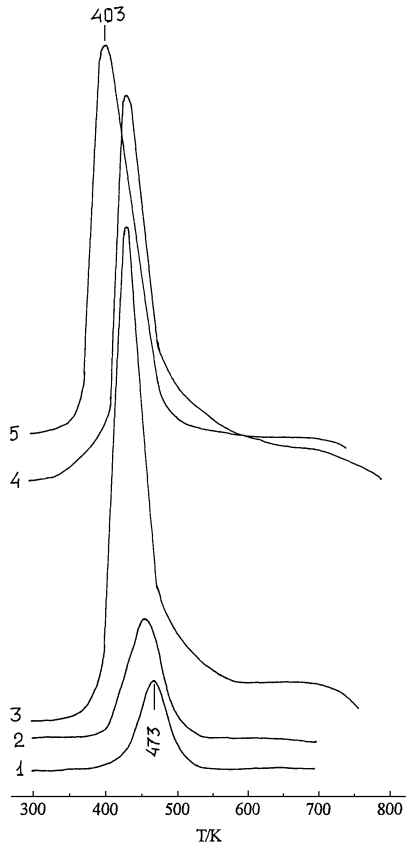

Figure 8. TPR profiles for dehydration of isopropyl alcohol in the case of AB (**1**), ABF005 (**2**), ABF01 (**3**; at a 1:2 scale), ABF05 (**4**), ABF1 (**5**) heat-treated at 673 K

under investigation are active also in the reaction of dealkylation of cumene, with T_{max} for the benzene release being equal to 783 K and 893 K.

According to the IR spectroscopy data for pyridine adsorbed on the synthesized aluminium borates, the concentration of surface B-acid sites is insignificant, therefore, the differences in the catalytic activity of these substances can be related mainly to changes in their L-acidity.

Our studies of the catalytic activity of aluminium borates give evidence that in comparison with the starting amorphous aluminium borate the catalytic activity of ABF005 in the reaction of dehydration of isopropyl alcohol increases slightly. Due to the small content of F^- in the sample, the structure of acid sites changes insufficiently, so that the influence on the activity of the material is limited. The highest activity of ABF01 is observed in the alcohol conversion (Fig. 8). This can be explained by an increase in the strength of L-sites, as well as by a small decrease in their number (see the discussion of the IR spectroscopy experiment). The catalytic activity of ABF05 and ABF1 is smaller, due to some decrease in the concentration of surface L-sites Al^{3+} (Fig. 6). It is also evident that in the case of the fluorine-containing samples T_{max} for the propylene release is shifted into the low-temperature region, because of the total increase in the fraction of strong L-acid sites.

CONCLUSIONS

Impregnating aluminium borates with NH_4F one can synthesize amorphous fluorine-containing aluminium borates with a high surface area. The amorphous materials of this type with a large content of F^- (> 10–15 wt.%) cannot be prepared. With the increasing F^- content in amorphous samples, the temperature of their crystallization is decreased. The IR spectroscopy study of adsorption of pyridine on the surface of aluminium borates shows the presence of L- and B-acid sites. The Brönsted acidity seems to be due to B–OH groups and F^-, as it was the case for fluorinated Al_2O_3 [33]. Lewis acidity is attributed to coordinatively unsaturated Al^{3+} and B^{3+} (in the F^- environment). The activity of the fluorine-containing materials in the reaction of dehydration of isopropyl alcohol is higher than that in the case of the starting aluminium borate. It is evident that the high catalytic activity of fluorine-containing catalysts may be explained by introduction of F^- into the aluminium borate matrix. Acid-base properties of the aluminium borates synthesized can be adjusted by varying the content of F^- in the samples. The results achieved provide evidence for the fact that samples whose F^- content amounts to 1.5–3.0 wt.% should be the most active catalysts.

REFERENCES

1. Gielisse P.J.M. and Foster W.R., *Nature,* **195**, 79 (1962).
2. Scholze H., *Z. Anorg. Allg. Chem.,* **284**, 272 (1956).
3. Yamaguchi O., Tada M., Takeoka K. and Shimizu K., *Bull. Chem. Soc. Japan,* **52**, 2153 (1979).

4. Capponi J., Chenavas J. and Joubert J., *Bull. Soc. Franc. Miner. et Cristallogr.,* **95**, 412 (1972).
5. Reynaud C., *Bull. Soc. Franc. Miner. et Cristallogr.,* **100**, 28 (1977).
6. Tsai M.E. and Chen Y.M., *Catal. Lett*., **6**, 225 (1990).
7. Tanabe S., Hirao K., Soga N. and Hanada T., *J. Solid State Chem*., **97**, 481 (1992).
8. Bechara R., Aboukais A. and Bonnelle J.P., *J. Chem. Soc., Farad. Trans*., **89**, 1257 (1993).
9. Hriljak J.A., Brown R.D., Cheethan A.K. and Satek L.C., *J. Solid State Chem*., **84**, 289 (1990).
10. Izumi Y. and Shiba T., *ibid.,* **67**, 559 (1964).
11. Mochida I., Anju Y., Kato A. and Seiyama T., *Bull. Chem. Soc. Jap.,* **43**, 2245 (1970).
12. Mochida I., Anju Y., Kato A. and Seiyama T., *J. Catal.,* **21**, 263 (1971).
13. Sato S., Asebe S., Urabe H. and Izumi Y., *Appl. Catal.,* **29**, 107 (1987).
14. Lehmann H.A. and Teske K., *Z. Anorg. Allg. Chem.,* **400**, 169 (1973).
15. Teske K. and Lehmann H.A., *Z. Chem.,* **6**, 230 (1966).
16. Peil K.P., Galya L.G. and Marcelin G., *J. Catal.,* **115**, 441 (1989).
17. Delmastro A., Gozzelino G., Mazza D., Vallino M., Busca G. and Lorenzelli V.*, J. Chem. Soc., Farad. Trans.,* **14**, 2065 (1992).
18. Simon S., van der Pol A., Reijerse E.J., Kentgens A.P.M., van Moorsel G.J. and de Boer E., *J. Chem. Soc., Farad. Trans.,* **18**, 2663 (1994).
19. Wang J., Feng S. and Xu R., *J. Chem. Soc., Chem. Commun.,* **5**, 265 (1989).
20. Yu J., Xu R., Kan Q., Xu Y. and Xu B., *J. Mater. Chem.,* **1**, 77 (1993).
21. Xu B., Cai T., Yu J., Xiao F., Xu R., Huang J. and Xu Y., *J. Chem. Soc., Chem. Commun.,* **13**, 1228 (1992).
22. Yu J., Tu K. and Xu R., in *Studies in Surface Science and Catalysis,* eds. J. Weitkamp, H.G. Karge, H. Pfeifer, W. Holderich, Amsterdam, 1994, **84A**, p. 315.
23. Brichka S.Ya. and Brei V.V., *Mendeleev Commun.,* **3**, 125 (1997).
24. Brichka S.Ya., Brei V.V. and Chuiko A.A., *Z. Prikl. Khim.*, **70**, 1447 (1997).
25. Yamaguchi O., Tada M., Takeoka K. and Shimizu K., *Bull.Chem. Soc.Japan,* **52**, 2153 (1979).
26. Nakamoto K., *Infrared and Raman Spectra of Inorganic and Coordination Compounds*, Wiley, N.Y., 1986.
27. Weir C.E., *J. Res. Nat. Bur. Stand*., **70A**, 153 (1966).
28. Paukshtis E.A., *Infrared Spectroscopy in Heterogeneous Acid-Base Catalysis,* Nauka, Novosibirsk, 1992.
29. Pelmenschikov A.G., van Santen R.A., Janchen J. and Meijer E., *J. Phys. Chem*., **97**, 11071 (1993).
30. Zenkovets G.A., Tarasova D.V., Paukshtis E.A. and Nikoro T.A., *React. Kinet. Catal. Lett*., **18**, 301 (1981).
31. Zidomirov G.M. and Pelmenschikov A.G., *Z. Struct.Chem.*, **27**, 150 (1986).
32. Peri J.B., *ibid,* **72**, 2917 (1986).
33. Corma A., Fornes V. and Ortega E., *J. Catal.,* **92**, 284 (1985).
34. Corma A., *Chem. Rev.,* **95**, 559 (1995).
35. Brei V.V., Kaspersky V.A., Khomenko K.N. and Chuiko A.A., *Adsorption Science & Technology,* **14**, 349 (1996).
36. Kislyuk M.U. and Rozanov V.V., *Kinetics and Catalysis*, **36**, 89 (1995).
37. Kibby C.L. and Hall W.K., *J. Catal*., **29**, 144 (1973).